Available online at www.sciencedirect.com
ScienceDirect
Tetrahedron
Tetrahedron 64 (2008) 168–174
www.elsevier.com/locate/tet

Structural effect of synthetic zwitterionic cosolutes on the stability of DNA duplexes

Kazuya Koumoto [a], Hirofumi Ochiai [a], Naoki Sugimoto [a,b,*]

[a] *Frontier Institute for Biomolecular Engineering Research (FIBER), Konan University, 8-9-1 Okamoto, Higashinada-ku, Kobe 658-8501, Japan*

[b] *Department of Chemistry, Faculty of Science and Engineering, Konan University, 8-9-1 Okamoto, Higashinada-ku, Kobe 658-8501, Japan*

Received 12 September 2007; received in revised form 16 October 2007; accepted 18 October 2007
Available online 22 October 2007

Abstract

The molecular design of useful cosolutes for polymerase chain reaction (PCR), which is one of the most important techniques in molecular biology, plays a significant role in amplification of highly stable genome sequences because during PCR, strand dissociation sometimes fails due to high melting temperature. Here, we designed and synthesized eight new zwitterionic cosolutes derived from glycine betaine, a destabilizing reagent for GC-rich DNA duplexes, and systematically compared their ability to destabilize DNA duplexes and to amplify genome DNA by PCR. We found that introduction of *n*-butyl groups rather than methyl groups into the ammonium group reduced the melting temperature of DNA duplexes 11-fold more than what was observed for the scaffold cosolute, glycine betaine, and furthermore, the cosolute can amplify the stable genome sequence by PCR.

Keywords: Polymerase chain reaction; Compatible solutes; Betaine; Synthetic cosolutes

1. Introduction

Polymerase chain reaction (PCR)[1] is one of the most important techniques in molecular biology. Despite its wide application, however, it is still the case that the reaction sometimes fails to produce the target products.[2] Accordingly, improvements in the conditions for PCR are required. It has been reported that the presence of organic molecules such as dimethylsulfoxide (DMSO),[3–5] glycerol,[4,5] formamide,[5,6] glycine betaine,[5,7] and L-ectoine[8] can improve the yield of the target product. In particular, cellular organic molecules such as glycine betaine and L-ectoine, collectively referred to as compatible solutes, can enhance efficiency much more than other molecules. This has been attributed to the observation that compatible solutes reduce the melting temperature of DNA duplexes without resulting in a significant deformation of DNA polymerase[9,10] and facilitate the initial strand dissociation process that occurs during each PCR cycle.

Compatible solutes are produced by metabolism of saccharides, amino acids, and lipids in the cell and are known to regulate an osmotic gradient in the cytoplasm, enabling cells to survive in extremely harsh environments.[11] To date, many compatible solutes have been identified,[12] including glycerol, *myo*-inositol, sorbitol, diglycerol phosphate, glycine, proline, glycine betaine, proline betaine, L-ectoine, taurine, hypotaurine, glycerophosphorylcholine, choline-*O*-sulfate, and others (Fig. 1). Most of these have both cationic and anionic charges in their structures and the charged structure seems to regulate stability, conformation, and activity of various biomolecules in cells.[13] Although the detailed mechanism is still unclear, the results of various studies suggest that the effect of a cosolute on the stability of biomolecules is related to an indirect interaction via water molecules rather than via direct interaction between the target molecule and the compatible solutes themselves.[10,14,15]

* Corresponding author. Tel.: +81 78 435 2497; fax: +81 78 435 2766.
E-mail address: sugimoto@konan-u.ac.jp (N. Sugimoto).

0040-4020/$ - see front matter © 2007 Elsevier Ltd. All rights reserved.
doi:10.1016/j.tet.2007.10.060

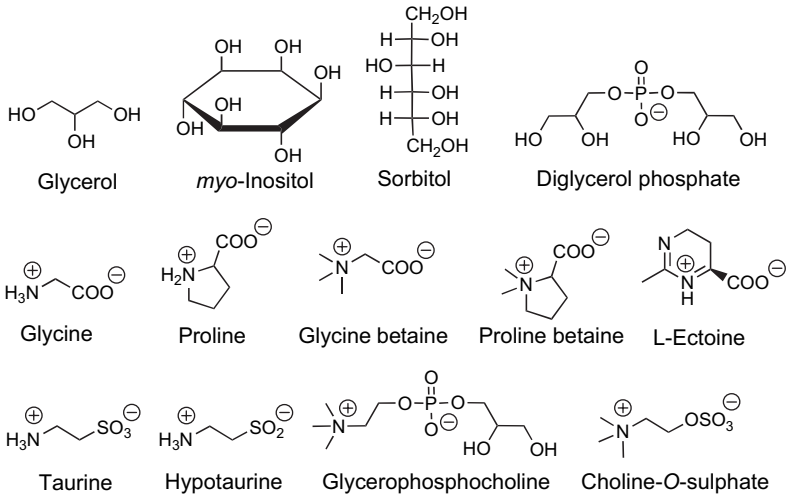

Figure 1. Chemical structures of compatible solutes.

Successful design of new compatible solutes (cosolutes) may be useful for application in PCR-based experiments. In spite of this promising property, however, no systematic studies that relate the structure of compatible solutes to their effects on the stability of DNA duplexes except for those of amide[6] and sulfone[16] derivatives that are not compatible solutes have been reported, which is likely due to the difficulty of synthesizing and purifying cosolutes. In this work, we have developed a synthetic method for production of zwitterionic cosolutes from glycine betaine and systematically compared the effects of the synthetic cosolutes on the stability of DNA duplexes and the amplification of PCR.

2. Results and discussion

2.1. Molecular design of zwitterionic cosolutes

We selected glycine betaine as a scaffold for developing zwitterionic cosolutes because it has been used previously as a cosolute for PCR, specifically in amplification of GC-rich genome sequences.[5,7] In the structure of glycine betaine (**1**) (Fig. 2), a trimethylammonium cation and a carboxylate anion are linked by a methylene (C_1) spacer. To investigate the importance of the chemical structure of glycine betaine (**1**), we designed eight new zwitterionic cosolutes (**2**–**9**) (Fig. 2). Compounds **2** and **3** have a spacer that is longer than the spacer in glycine betaine (**1**); they have C_3 and C_5 spacers, respectively. Compounds **4**, **5**, and **6** differ in terms of the bulkiness of the ammonium group; these compounds have triethylammounim, tri-*n*-propylammonium, and tri-*n*-butylammonium groups, respectively. For compounds **7** and **8**, hydrophilic (morpholine) or hydrophobic (piperidine) cyclic groups were introduced into the ammonium group. Compound **9** contains two zwitterionic groups in a single molecule. Using all of the zwitterionic cosolutes, we next systematically investigated how differences in the structures of the cosolutes change their ability to destabilize DNA duplexes.

2.2. Synthesis of cosolutes

Cosolutes with one zwitterionic group (**2**–**8**) were synthesized as shown in Scheme 1. In brief, (i): trialkylamine was slowly added to ethyl bromo-alkylate dissolved in ethyl acetate, and the solution was stirred vigorously for 1 day. The precipitate produced during the reaction was filtered and recrystallized with the ethanol/ethyl acetate mixture. White crystals were obtained at a yield of 77–96% (**2a**–**8a**). The cosolute with two zwitterionic groups (**9**) was synthesized similarly except that ethanol as the solvent instead of ethyl acetate (Scheme 1 (ii)). The product (**9a**) was obtained at a yield of 69%. Hydrolysis of the ethyl ester and removal of the counteranion present in precursors (**2a**–**9a**) was achieved by anion-exchange chromatography (Amberite IR-402). After thoroughly drying the samples in vacuo using P_2O_5, each zwitterionic cosolute (**2**–**9**) was obtained as highly hygroscopic solid. Hydrolysis of the ester group and desalination were observed, as we noted the disappearance of peaks derived from ester group using FTIR, ^{1}H NMR spectra to detect ester

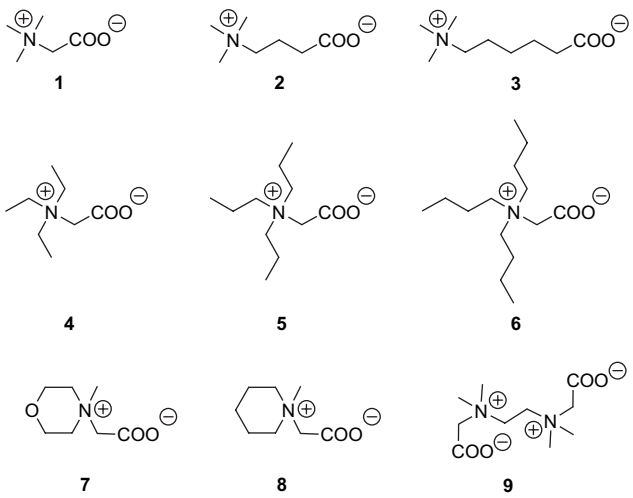

Figure 2. Chemical structures of synthetic zwitterionic cosolutes.

groups, and elemental analysis to detect salts. All the reactions and purifications proceeded in a simple way.

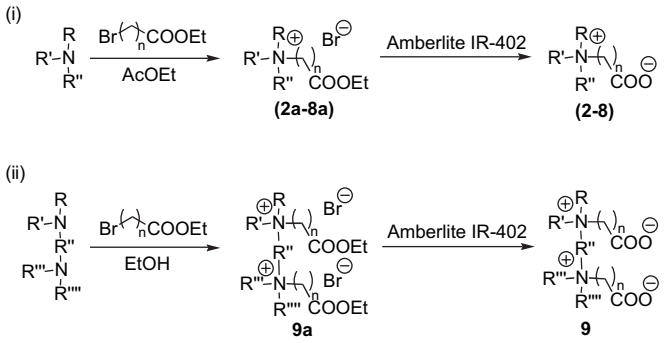

Scheme 1. Routes to synthesis of zwitterionic cosolutes.

Table 1
Comparison of T_m (°C) values of **DNA1**, **DNA2**, and **DNA3** in the absence and presence of 0.5 M cosolutes[a]

Cosolutes	DNA1	DNA2	DNA3
None	58.9±1.6	44.3±1.7	78.2±0.2
1	58.7±0.4	44.0±0.9	78.1±0.3
2	58.3±0.3	44.4±1.9	78.2±0.4
3	56.4±0.1	42.6±1.2	75.7±0.1
4	56.2±0.9	40.6±1.3	74.5±0.1
5	55.3±0.2	38.5±1.0	71.0±0.1
6	54.6±1.3	37.0±1.0	69.2±0.4
7	57.6±0.8	42.8±0.1	76.6±0.2
8	58.1±0.7	40.3±0.8	74.4±0.2
9	58.2±0.3	42.1±0.3	78.0±0.2

[a] Melting temperatures (T_m) were measured in 10 mM Tris buffer (pH 8.0) containing 100 mM NaCl and 0.5 M cosolutes. [**DNA1**]=40 μM, [**DNA2**]=40 μM, and $[\mathbf{DNA3}]_{total}$=20 μM.

2.3. Effect of synthetic cosolutes on the stability of DNA

The positive role of compatible solutes on PCR is to decrease the melting temperature (T_m) of DNA duplexes with high T_m.[5,7] To investigate how synthetic cosolutes affect the stability of DNA duplexes, T_m values of DNA duplexes were compared in the absence and presence of the cosolutes generated in this work. According to the standard PCR protocols, glycine betaine should be added to the reaction buffer at a concentration in the range 0.1–2.0 M.[5,7] Thus, we adjusted the cosolute concentration to 0.5 M in this study. For the DNA substrate, we selected two self-complementary 8mer DNA sequences (**DNA1**; 5′-CGGCGCCG-3′, **DNA2**; 5′-ATGCGCAT-3′) and one non-self-complementary 40mer DNA sequence (**DNA3**; 5′-GAAACCACAACGGTTACCTGACCATGTCTTGATACGATCG-3′/5′-CGATCGTATCAAGACATGGTCAGGTAACCGTTGTGGTTTC-3′). T_m values of the DNA duplexes were measured in 10 mM Tris buffer (pH 8.0) containing 100 mM NaCl. The shape of the melting curves in the presence of cosolute is similar to that in the absence of cosolute, indicating that the cosolutes do not induce notable conformational perturbation. The T_m values estimated from the melting curves for 40 μM **DNA1**, 40 μM **DNA2**, and 20 μM **DNA3** are summarized in Table 1. The change in T_m (ΔT_m) when UV melting was performed in the presence of cosolutes is shown in Figure 3. The ΔT_m values shown in Figure 3 were estimated using the following equation: $\Delta T_m = T_{m,\ cosolute} - T_{m,\ none}$, where $T_{m,\ cosolute}$ and $T_{m,\ none}$ are T_m values observed in the presence or absence of cosolute, respectively.

As shown in Figure 3, the ability of cosolutes to destabilize DNA duplexes is independent of the GC content or length of the duplexes, although the degree of destabilization induced by each cosolute differs. We next compared the effect of changing the length of the spacer, which sits between the cation and the anion of the cosolute, on DNA stability. Comparison of the ΔT_m values among cosolutes **1**, **2**, and **3** revealed that their destabilizing ability seems to depend on spacer length. A spacer length of less than C_3 scarcely altered DNA stability, whereas the degree of destabilization was mildly increased when the spacer length was longer than C_3, although the destabilizing ability remained relatively weak. In contrast, bulkiness of the ammonium groups considerably reduced DNA stability. As the alkyl chain was changed from methyl to ethyl, *n*-propyl or *n*-butyl, the ΔT_m values decreased greatly. For example, in the case of **DNA3**, ΔT_m for cosolute **1** is only −0.1 °C, whereas the ΔT_m values for cosolutes **4**, **5**, and **6** decreased to −3.7 °C, −7.2 °C, and −9.0 °C, respectively. This tendency was also observed for **DNA1** and **DNA2**. The results indicate that increasing the alkyl chains of the ammonium cation in a cosolute increases its ability to destabilize DNA duplexes.

Next, we changed the chemical structure of the alkyl chain and compared the destabilization effect of alkyl chains on duplex stability using cosolutes **7** and **8**. Cosolutes **7** and **8** have either a hydrophilic or a hydrophobic cyclic group at the ammonium group and their bulkiness (size) of ammonium group is similar to that of cosolute **4** (triethylammonium). In the case of **DNA3**, the ΔT_m for cosolute **7**, which has a polar oxygen atom outside the ammonium group, is −1.6 °C. On the other hand, that for cosolute **8** is −3.8 °C, consistent with the value for cosolute **4** (−3.7 °C). These results indicate that polar functional group outside of the ammonium group reduce the destabiling ability for DNA duplexes. Finally, we compared

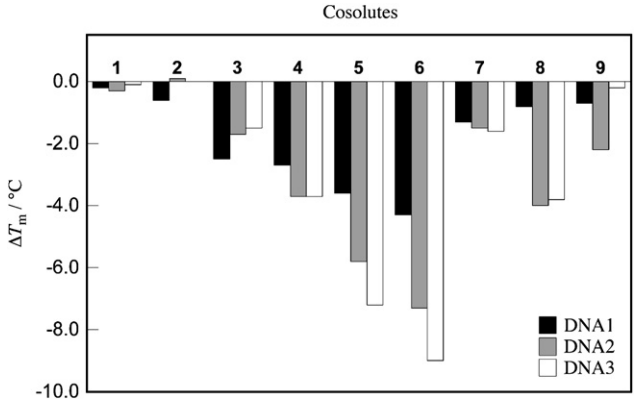

Figure 3. Comparison of the ability of synthetic cosolutes to destabilize **DNA1**, **DNA2**, and **DNA3**. ΔT_m values were estimated using the following equation ($\Delta T_m = T_{m,\ cosolute} - T_{m,\ none}$) with T_m values as shown in Table 1.

the effect of the number of zwitterionic groups present in a single molecule on the stability of DNA by comparing cosolutes **1** and **9**. The T_m values of DNA duplexes in the presence of cosolute **9** decreased 0.7 °C, 2.2 °C, and 0.2 °C for **DNA1**, **DNA2**, and **DNA3**, respectively, whereas those in the presence of cosolute **1** decreased 0.2 °C, 0.3 °C, and 0.1 °C for **DNA1**, **DNA2**, and **DNA3**, respectively. Although cosolute **9** destabilized DNA duplexes slightly better than cosolute **1**, the destabilization ability was not so large as compared with the effect of both linker length and bulkiness of the ammonium cation. When taken together with the present results, we conclude that introduction of an alkyl chain without polar functional group outside the ammonium group is the most important factor for destabilization of DNA duplexes by a cosolute.

*2.4. Comparison of the destabilizing ability of glycine betaine (cosolute **1**) and cosolute **6***

The above result shows that among the synthetic cosolutes assayed in this work, cosolute **6** is the most effective cosolute for bringing about a decrease in the melting temperature of DNA duplexes. To evaluate the destabilizing ability quantitatively, we plotted the T_m values of **DNA3** as a function of cosolute concentration using cosolute **1** as the reference (Fig. 4). As the cosolute concentration rises, the T_m value decreases linearly (Fig. 4). This behavior is identical to that reported in previous studies using other cosolutes.[8,17] Comparison of the slope revealed that the destabilizing ability of cosolute **6** was superior to that of cosolute **1**. For example, in order to reduce the T_m by 5 °C, cosolute **1** must be adjusted to a concentration of 2.3 M, whereas a concentration of 0.2 M of cosolute **6**, that is, one eleventh more dilute, has the same effect. It is noteworthy that only changing the alkyl chain from methyl to *n*-butyl groups induces a drastic change in the cosolutes' ability to destabilize a DNA duplex.

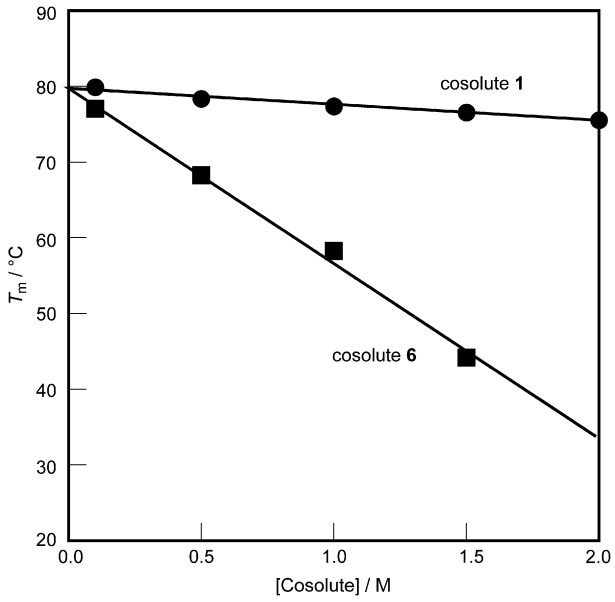

Figure 4. Plot of T_m values of **DNA3** as a function of the concentration of cosolute **1** (filled circle) and cosolute **6** (filled square).

*2.5. Comparison of the CD spectra of **DNA3** in the absence and presence of cosolute **6***

Although we clarified that the synthetic cosolutes effectively destabilize the DNA duplexes, the drastic decrement in the melting temperature of duplexes may be related to the conformational perturbation of the helical structure that prevents from forming the hydrogen bonding and stacking interactions. Therefore, to assess the duplex conformation in the presence of cosolute, we compared the circular dicroism (CD) spectra of 10 μM **DNA3** in the absence and presence of cosolute **6**. Figure 5 shows the CD spectra for **DNA3** itself (solid line) and with 0.5 M cosolute **6** (broken line) at 25 °C. Both CD spectra are completely identical with each other, indicating that the DNA duplexes still keep the B-form structure even in the presence of cosolutes. This result suggested that the synthetic cosolutes also show an intact property for biomolecules similar to glycine betaine (cosolute **1**) that indirectly interacts with biomolecules via water molecules.[10]

2.6. PCR experiments

Finally, to examine how the synthetic cosolute affect DNA amplification by PCR, we compared the amplification of a TNF-beta 27[18] in human genome DNA using a KOD−plus−Ver.2® polymerase. Cosolute **6** was used because it had the strongest destabilizing ability for DNA duplexes. Cosolute **1** (glycine betaine) was used as the control. To increase the melting temperature of TNF-beta 27, NaCl concentration was increased to be 70 mM in the buffer solution containing reaction buffer supplemented with KOD dash polymerase, 0.6 μM primers, 0.2 μM dNTP, 1.5 mM $MgSO_4$, 5 mM cosolute, and 12 ng genome DNA in 30 μl volume. Figure 6a shows the agarose gel pattern in the absence and the presence of

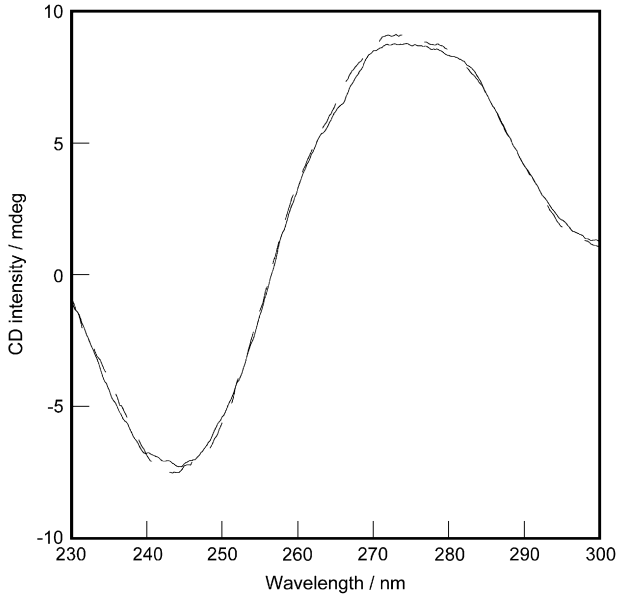

Figure 5. Circular dichroism spectra of **DNA3** (solid line) and it with 0.5 M cosolute **6** (broken line) at 25 °C. [**DNA3**]=10 μM, [Tris (pH 8.0)]=0.1 M, [NaCl]=0.1 M, and [cosolute **6**]=0 or 0.5 M.

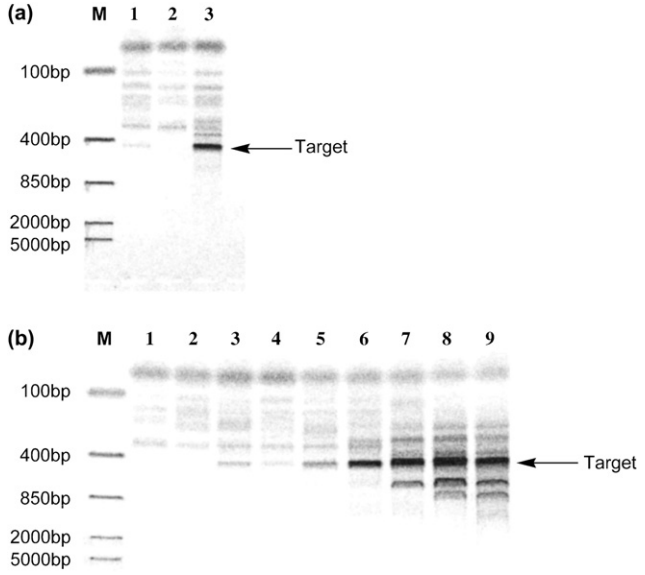

Figure 6. Effects of cosolutes on PCR amplification of TNF-beta 27 in human genome DNA. (a) PCR amplification of TNF-beta 27 in the absence and presence of cosolutes **1** and **6** (5 mM). Lane 1 (no cosolute), lane 2 (5 mM cosolute **1**), and lane 3 (5 mM cosolute **6**); (b) PCR amplification of TNF-beta 27 with addition of up to 1000 mM cosolute **1**. Lane 1 (5 mM), lane 2 (10 mM), lane 3 (30 mM), lane 4 (50 mM), lane 5 (100 mM), lane 6 (200 mM), lane 7 (400 mM), lane 8 (800 mM), and lane 9 (1000 mM).

cosolutes **1** and **6**, respectively. Only in the presence of 5 mM cosolute **6**, amplification of target product (434 bp) can be improved. On the other hand, in the absence and presence of cosolute **1**, no amplification can be observed. As shown in Figure 6b, amplification by cosolute **1** can be observed at the concentration more than 100 mM, that is, 20-fold higher than that of cosolute **6**. The present result evidenced that the synthetic cosolutes can improve the amplification of stable genome sequence to reduce the melting temperature.

3. Conclusion

We successfully synthesized zwitterionic cosolutes derived from glycine betaine. The results of UV experiments revealed that the zwitterionic cosolutes destabilize DNA duplexes in a manner consistent with their chemical structures. In particular, introduction of long alkyl chains without polar functional groups outside the ammonium group played a significant role in destabilization of DNA duplexes. Furthermore, the synthetic cosolutes can improve the amplification of stable genome sequences to reduce the melting temperature. Thus, we expect that the cosolutes will be useful for creating favorable conditions for PCR and other biomolecular reactions.

4. Experimental section

4.1. Syntheses

*4.1.1. 4-N,N,N-Trimethylammonium-butylic acid ethyl ester bromide (**2a**)*

Into a solution of 4-bromo-*n*-butylic acid ethyl ester (25.0 g, 0.13 mmol) in ethyl acetate (100 mL) was bubbled trimethylamine gas generated by heating a 40% trimethylamine solution (300 mL) and the mixture was stirred at rt for 1 day. The precipitate produced during the reaction was filtered. The residue was recrystallized with ethanol/ethyl acetate mixture and was dried in vacuo to give **2a** (26.4 g, 77%) as a white powder: FTIR (ATR) ν/cm^{-1} 2966, 1731, 1494, 1481, 1376, 1298, 1198, 1021, 963, 915, 755; ^1H NMR (500 MHz, DMSO-d_6) δ/ppm 1.18 (t, J=7.3 Hz, 3H), 1.92 (m, 2H), 2.37 (t, J=7.3 Hz, 2H), 3.05 (s, 9H), 3.27 (m, 2H), 4.07 (q, J=7.2 Hz, 2H). Elemental Analysis: Calculated for $C_9H_{20}BrNO_2\cdot 0.1H_2O$: C, 42.23%; H, 7.97%; N, 5.47%. Found: C, 42.23%; H, 8.08%; N, 5.51%.

*4.1.2. 6-N,N,N-Trimethylammonium-hexanoic acid ethyl ester bromide (**3a**)*

Compound **3a** was obtained in 92% yield as a white powder in the same way as for the preparation of **2a**: FTIR (ATR) ν/cm^{-1} 3494, 2954, 1733, 1719, 1485, 1375, 1181, 1130, 1041, 974, 919, 864, 739; ^1H NMR (500 MHz, DMSO-d_6) δ/ppm 1.17 (t, 3H), 1.25 (t, 2H), 1.55 (m, 2H), 1.66 (t, 2H), 2.31 (br s, 2H), 3.03 (s, 9H), 3.26 (m, 2H), 4.04 (q, J=7.2 Hz, 2H). Elemental Analysis: Calculated for $C_{11}H_{24}BrNO_2\cdot 0.2H_2O$: C, 46.22%; H, 8.62%; N, 4.90%. Found: C, 46.40%; H, 8.94%; N, 4.99%.

*4.1.3. 2-N,N,N-Triethylammonium-acetic acid ethyl ester bromide (**4a**)*

To a solution of triethylamine (100 mL) in ethyl acetate (100 mL) cooled to 4 °C was added 2-bromoacetic acid ethyl ester (37.5 g, 0.22 mol) and the mixture was stirred at rt for 1 day. Precipitate produced during the reaction was filtered. The residue was recrystallized by ethanol/ethyl acetate and was dried in vacuo to give **4a** (50.2 g, 86%) as a white powder: FTIR (ATR) ν/cm^{-1} 2991, 1739, 1446, 1217, 1176, 1032, 859, 817; ^1H NMR (500 MHz, DMSO-d_6) δ/ppm 1.22 (t, J=7.0 Hz, 9H), 1.25 (t, J=7.5 Hz, 3H), 3.49 (q, J=7.3 Hz, 6H), 4.23 (q, J=7.2 Hz, 2H), 4.35 (s, 2H). Elemental Analysis: Calculated for $C_{10}H_{22}BrNO_2\cdot 0.3H_2O$: C, 43.90%; H, 8.34%; N, 5.12%. Found: C, 43.83%; H, 8.22%; N, 5.10%.

*4.1.4. 2-N,N,N-Tri-n-propylammonium-acetic acid ethyl ester bromide (**5a**)*

Compound **5a** was obtained in 67% yield as a white powder in the same way as for the preparation of **4a**: FTIR (ATR) ν/cm^{-1} 2968, 1743, 1440, 1407, 1212, 1167, 1028, 943, 746; ^1H NMR (500 MHz, DMSO-d_6) δ/ppm 0.90 (t, J=7.0 Hz, 9H), 1.26 (t, J=7.5 Hz, 3H), 1.66 (br s, 6H), 3.40 (br s, 6H), 4.22 (m, 2H), 4.38 (s, 2H). Elemental Analysis: Calculated for $C_{13}H_{28}BrNO_2$: C, 50.32%; H, 9.10%; N, 4.51%. Found: C, 50.04%; H, 9.00%; N, 4.49%.

*4.1.5. 2-N,N,N-Tri-n-butylammonium-acetic acid ethyl ester bromide (**6a**)*

Compound **6a** was obtained in 80% yield as a white powder in the same way as for the preparation of **4a**: FTIR (ATR) ν/cm^{-1} 2961, 1741, 1468, 1207, 1043, 872, 745; ^1H NMR (500 MHz, DMSO-d_6) δ/ppm 0.93 (t, J=7.5 Hz, 9H), 1.25 (t,

J=7.6 Hz, 3H), 1.30 (q, J=7.3 Hz, 6H), 1.62 (m, 6H), 3.43 (m, 6H), 4.23 (q, J=7.0 Hz, 2H), 4.38 (s, 2H). Elemental Analysis: Calculated for $C_{16}H_{34}BrNO_2 \cdot 0.2H_2O$: C, 53.98%; H, 9.76%; N, 3.93%. Found: C, 53.78%; H, 9.69%; N, 4.06%.

*4.1.6. 2-(1-Methyl-morpholinium-1-yl)-acetic acid ethyl ester bromide (**7a**)*

Compound **7a** was obtained in 95% yield as a white powder in the same way as for the preparation of **4a**: FTIR (ATR) ν/cm^{-1} 2974, 1731, 1471, 1416, 1226, 1122, 1030, 909; ^{1}H NMR (500 MHz, DMSO-d_6) δ/ppm 1.27 (t, J=8.8 Hz, 9H), 3.40 (s, 3H), 3.64 (m, 2H), 3.71 (m, 2H), 3.98 (m, 4H), 4.26 (q, J=8.4 Hz, 2H), 4.72 (s, 2H). Elemental Analysis: Calculated for $C_9H_{18}BrNO_3 \cdot 0.1H_2O$: C, 40.04%; H, 6.81%; N, 5.19%. Found: C, 39.91%; H, 6.81%; N, 5.19%.

*4.1.7. 2-(1-Methyl-piperidinium-1-yl)-acetic acid ethyl ester bromide (**8a**)*

Compound **8a** was obtained in 96% yield as a white powder in the same way as for the preparation of **4a**: FTIR (ATR) ν/cm^{-1} 2945, 1738, 1444, 1214, 1058, 1014, 944, 909, 745; ^{1}H NMR (500 MHz, DMSO-d_6) δ/ppm 1.23 (t, J=7.3 Hz, 3H), 1.51 (m, 2H), 1.81 (m, 4H), 3.21 (s, 3H), 3.50 (m, 2H), 3.58 (m, 2H), 4.21 (q, J=7.2 Hz, 2H), 4.50 (s, 2H). Elemental Analysis: Calculated for $C_{10}H_{20}BrNO_2$: C, 45.12%; H, 7.57%; N, 5.26%. Found: C, 45.01%; H, 7.64%; N, 5.26%.

*4.1.8. 1,2-Bis{[N,N-dimethyl-N-(acetic acid ethyl ester-1-yl)]-ammonium-N-yl}ethane dibromide (**9a**)*

To a solution of *N*,*N*,*N*′,*N*′-tetramethylethylene diamine (25.0 g) in ethanol (400 mL) cooled to 4 °C was added bromoacetic acid (100 mL) and the mixture was stirred at rt for 4 days. Precipitate produced during the reaction was filtered. The residue was washed by ethanol with ultrasonication and was dried in vacuo to give **9a** (66.6 g, 69%) as a white powder: FTIR (ATR) ν/cm^{-1} 3008, 1745, 1469, 1382, 1241, 1208, 1142, 1014, 913, 856, 764; ^{1}H NMR (500 MHz, DMSO-d_6) δ/ppm 1.28 (t, J=7.0 Hz, 6H), 3.34 (s, 12H), 4.19 (s, 4H), 4.26 (q, J=7.2 Hz, 4H), 4.58 (s, 4H). Elemental Analysis: Calculated for $C_{14}H_{30}Br_2N_2O_4$: C, 37.35%; H, 6.72%; N, 6.22%. Found: C, 37.37%; H, 6.72%; N, 6.22%.

*4.1.9. 4-N,N,N-Trimethylammonium-butylate (**2b**)*

Compound **2a** (23.7 g, 0.09 mol) dissolved in water (20 mL) was passed through ion-exchange chromatography (Amberite IR-402CL). The eluting solution was evaporate at 45 °C to dryness and the white solid was dried in vacuo using P_2O_5 to give **2b** (13.2 g, 100%) as a white powder: FTIR (ATR) ν/cm^{-1} 3338, 3037, 2964, 1580, 1488, 1397, 1335, 968, 932, 762; ^{1}H NMR (500 MHz, DMSO-d_6) δ/ppm 1.75 (m, 2H), 1.80 (m, 2H), 3.02 (s, 9H), 3.25 (m, 2H), 3.38 (s, 9H). Elemental Analysis: Calculated for $C_7H_{15}NO_2 \cdot 0.1H_2O$: C, 57.19%; H, 10.44%; N, 9.53%. Found: C, 56.93%; H, 10.44%; N, 9.50%.

*4.1.10. 6-N,N,N-Trimethylammonium-hexanate (**3b**)*

Compound **3b** was obtained quantitatively as a white powder in the same way as for the preparation of **2b**: FTIR (ATR) ν/cm^{-1} 2954, 1567, 1507, 1490, 1375, 909, 753; ^{1}H NMR (300 MHz, DMSO-d_6) δ/ppm 1.22 (m, 2H), 1.43 (m, 2H), 1.62 (m, 2H), 1.76 (t, J=7.1 Hz, 2H), 3.02 (s, 9H), 3.24 (m, 2H). Elemental Analysis: Calculated for $C_9H_{19}NO_2 \cdot 0.15H_2O$: C, 61.43%; H, 11.08%; N, 7.96%. Found: C, 61.16%; H, 10.79%; N, 7.96%.

*4.1.11. 2-N,N,N-Triethylammonium-acetate (**4b**)*

Compound **4b** was obtained quantitatively as a white powder in the same way as for the preparation of **2b**: FTIR (ATR) ν/cm^{-1} 3508, 2992, 1633, 1606, 1479, 1343, 1162, 1015, 984, 803, 736; ^{1}H NMR (500 MHz, DMSO-d_6) δ/ppm 1.13 (br s, 9H), 3.38 (s, 2H), 3.46 (br s, 6H). Elemental Analysis: Calculated for $C_8H_{17}NO_2 \cdot 0.1H_2O$: C, 59.67%; H, 10.79%; N, 8.70%. Found: C, 59.75%; H, 10.96%; N, 8.80%.

*4.1.12. 2-N,N,N-Tri-n-propylammonium-acetate (**5b**)*

Compound **5b** was obtained in 65% yield as a white powder in the same way as for the preparation of **2b**: FTIR (ATR) ν/cm^{-1} 3390, 2973, 1632, 1476, 1337, 1308, 947, 851, 718; ^{1}H NMR (500 MHz, DMSO-d_6) δ/ppm 0.87 (t, J=7.0 Hz, 9H), 1.59 (m, 6H), 3.35 (s, 3H), 3.40 (m, 6H), 3.44 (s, 2H). Elemental Analysis: Calculated for $C_{11}H_{23}NO_2 \cdot 0.3H_2O$: C, 63.91%; H, 11.53%; N, 6.78%. Found: C, 64.05%; H, 11.88%; N, 6.85%.

*4.1.13. 2-N,N,N-Tri-n-butylammonium-acetate (**6b**)*

Compound **6b** was obtained quantitatively as a white powder in the same way as for the preparation of **2b**: FTIR (ATR) ν/cm^{-1} 3407, 2956, 2872, 1629, 1472, 1352, 1145, 1307, 867, 712; ^{1}H NMR (300 MHz, DMSO-d_6) δ/ppm 0.91 (t, J=7.2 Hz, 9H), 1.26 (m, 6H), 1.54 (m, 6H), 3.33 (s, 2H), 3.41 (m, 6H). Elemental Analysis: Calculated for $C_{14}H_{29}NO_2 \cdot 0.4H_2O$: C, 67.10%; H, 12.01%; N, 5.59%. Found: C, 66.98%; H, 11.81%; N, 5.67%.

*4.1.14. 2-(1-Methyl-morpholinium-1-yl)-acetate (**7b**)*

Compound **7b** was obtained quantitatively as a white powder in the same way as for the preparation of **2b**: FTIR (ATR) ν/cm^{-1} 2971, 1629, 1367, 1328, 1276, 1117, 1067, 905, 878; ^{1}H NMR (500 MHz, DMSO-d_6) δ/ppm 3.29 (s, 3H), 3.48 (m, 2H), 3.71 (m, 2H), 3.88 (br s, 4H). Elemental Analysis: Calculated for $C_7H_{13}NO_3 \cdot 0.1H_2O$: C, 52.22%; H, 8.28%; N, 8.70%. Found: C, 51.95%; H, 8.36%; N, 8.72%.

*4.1.15. 2-(1-Methyl-piperidinium-1-yl)-acetate (**8b**)*

Compound **8b** was obtained quantitatively as a white powder in the same way as for the preparation of **2b**: FTIR (ATR) ν/cm^{-1} 3479, 2943, 1621, 1482, 1370, 1330, 1031, 876, 798; ^{1}H NMR (500 MHz, DMSO-d_6) δ/ppm 1.50 (m, 2H), 1.74 (br s, 4H), 3.17 (s, 3H), 3.37 (m, 2H), 3.56 (s, 2H), 3.64 (m, 2H). Elemental Analysis: Calculated for $C_8H_{15}NO_2 \cdot 0.1H_2O$: C, 60.42%; H, 9.65%; N, 8.81%. Found: C, 60.26%; H, 9.45%; N, 8.85%.

*4.1.16. 1,2-Bis{[N,N-dimethyl-N-(acetate-1-yl)]ammonium-N-yl}ethane (**9b**)*

Compound **9b** was obtained quantitatively as a white powder in the same way as for the preparation of **2b**: FTIR (ATR) ν/cm^{-1} 3032, 1627, 1491, 1386, 1329, 1292, 895, 723; ^{1}H NMR (500 MHz, DMSO-d_6) δ/ppm 3.16 (s, 12H), 3.59 (s, 4H), 4.07 (s, 4H). Elemental Analysis: Calculated for $C_{10}H_{20}N_2O_4\cdot 0.2H_2O$: C, 50.91%; H, 8.73%; N, 11.88%. Found: C, 50.75%; H, 8.93%; N, 11.87%.

4.2. Materials

High performance liquid chromatography (HPLC) grade deoxyoligonucleotides (**DNA1**; 5′-CGGCGCCG-3′, **DNA2**; 5′-ATGCGCAT-3′, **DNA3**; 5′-GAAACCACAACGGTTACCT GACCATGTCTTGATACGATCG-3′/5′-CGATCGTATCAAGA CATGGTCAGGTAACCGTTGTGGTTTC-3′) were purchased from Hokkaido System Science Ltd. (Sapporo, Japan).

4.3. UV measurements

UV experiments using a Shimadzu 1700 spectrophotometer (Shimadzu, Kyoto, Japan) connected to a thermo-programmer were performed at temperature range from 0 to 95 °C. At low temperature range, the cuvette-holding chamber was flushed with a constant stream of dry N_2 gas to avoid condensation of water on the cuvette exterior. Before the measurements, the samples were heated to 95 °C, gently cooled to 4 °C at a rate of 2 °C min^{-1} and incubated at 4 °C for 1 h. UV melting curves of DNA samples in the absence and presence of cosolutes at 260 nm were obtained at a heating rate of 0.5 °C min^{-1}.

4.4. CD measurements

CD experiments using a JASCO spectropolarimeter (JASCO, Tokyo, Japan) connected to a thermo-programmer were performed at 25 °C. Before the measurements, the samples were heated to 95 °C, gently cooled to 4 °C at a rate of 2 °C min^{-1} and incubated at 4 °C for 1 h.

4.5. Purification of human genomic DNA

Human genomic DNA was prepared from oral mucosa. The genomic DNA from mucosal smear was purified with DNeasy® Tissue Kit (QIAGEN, Germany).

4.6. PCR experiments

PCR experiments were carried out in a total volume of 30 μL on a PC818 Program Temperature Control System (ASTEC, Fukuoka, Japan) with a 5 min 96 °C predenaturation; 40 cycles of 15 s at 98 °C, 45 s at 56 °C, 90 s at 72 °C, and 10 min at 72 °C final extension. Analysis of PCR products was done by 2.0% agarose electrophoresis. Staining was with Sybr gold. Pictures of the stained gels were taken with a FLA-5100 Image Analyzer (FUJI FILM Co. Ltd., Japan).

Acknowledgements

We thank Kaori Tsubaki for measuring UV melting, CD spectra, and PCR experiments. This work was supported in part by Grants-in-Aid for Scientific Research and the 'Academic Frontier' Project (2004–2009) from MEXT, Japan.

References and notes

1. Mullis, K. B. *Angew. Chem., Int. Ed. Engl.* **1994**, *33*, 1209–1213.
2. (a) Innis, M. A.; Myambo, K. B.; Gelfand, D. H.; Brow, M. A. *Proc. Natl. Acad. Sci. U.S.A.* **1988**, *85*, 9436–9440; (b) Reysenbach, A.-L.; Giver, L. J.; Wickham, G. S.; Pace, N. R. *Appl. Environ. Microbiol.* **1992**, *58*, 3417–3418.
3. (a) Winship, P. R. *Nucleic Acids Res.* **1989**, *17*, 1266; (b) Meeker, A. K.; Li, Y.-K.; Shortle, D.; Stites, W. E. *BioTechniques* **1993**, *15*, 372–374.
4. Pomp, D.; Medrano, J. F. *BioTechniques* **1991**, *10*, 58–59.
5. (a) Chakrabarti, R.; Schutt, C. E. *BioTechniques* **2002**, *32*, 866–874; (b) Ralser, M.; Querfurth, R.; Warnatz, H.-J.; Lehrach, H.; Yaspo, M.-L.; Krobitsch, S. *Biochem. Biophys. Res. Commun.* **2006**, *347*, 747–751.
6. Chakrabarti, R.; Schutt, C. E. *Nucleic Acids Res.* **2001**, *29*, 2377–2381.
7. Henke, W.; Herdel, K.; Jung, K.; Schnorr, D.; Loening, S. A. *Nucleic Acids Res.* **1997**, *25*, 3957–3958.
8. Schnoor, M.; Voß, P.; Cullen, P.; Boking, T.; Galla, H.-J.; Galinski, E. A.; Lorkowski, S. *Biochem. Biophys. Res. Commun.* **2004**, *322*, 867–872.
9. (a) Rees, W. A.; Yager, T. D.; Korte, J.; von Hippel, P. H. *Biochemistry* **1993**, *32*, 137–144; (b) Santoro, M. M.; Liu, Y.; Khan, S. M. A.; Hou, L.-X.; Bolen, D. W. *Biochemistry* **1992**, *31*, 5278–5283.
10. (a) Countenay, E. S.; Capp, M. W.; Anderson, C. F.; Record, M. T., Jr. *Biochemistry* **2000**, *39*, 4455–4471; (b) Felitsky, D. J.; Cannon, J. G.; Capp, M. W.; Hong, J.; Van Wynsberghe, A. W.; Anderson, C. F.; Record, M. T., Jr. *Biochemistry* **2004**, *43*, 14732–14743; (c) Hong, J.; Capp, M. W.; Anderson, C. F.; Saecker, R. M.; Felitsky, D. J.; Anderson, M. W.; Record, M. T., Jr. *Biochemistry* **2004**, *43*, 14744–14758.
11. (a) Wood, J. M. *Microbiol. Mol. Biol. Rev.* **1999**, *63*, 230–262; (b) Csonka, L. N. *Microbiol. Rev.* **1989**, *53*, 121–147.
12. (a) Parker, J. C. *Am. J. Physiol.* **1993**, *265*, C1191–C1200; (b) Yancey, P. H. *Amer. Zool.* **2001**, *41*, 699–709; (c) Yancey, P. H. *J. Exp. Biol.* **2005**, *208*, 2819–2830.
13. Minton, A. P. *J. Biol. Chem.* **2001**, *276*, 10577–10580.
14. (a) Nakano, S.; Karimata, H.; Ohmichi, T.; Kawakami, J.; Sugimoto, N. *J. Am. Chem. Soc.* **2004**, *126*, 14330–14331; (b) Miyoshi, D.; Karimata, H.; Sugimoto, N. *J. Am. Chem. Soc.* **2006**, *128*, 7957–7963; (c) Spink, C. H.; Charies, J. B. *Biochemistry* **1999**, *38*, 496–508; (d) Goobes, R.; Kahana, N.; Cohen, O.; Minsky, A. *Biochemistry* **2003**, *42*, 2431–2440.
15. Nordstrom, L. J.; Clark, C. A.; Andersen, B.; Champlin, S. M.; Schwinefus, J. J. *Biochemistry* **2006**, *45*, 9604–9614.
16. Chakrabarti, R.; Schutt, C. E. *Gene* **2001**, *274*, 293–298.
17. Spink, C. H.; Chaires, J. B. *J. Am. Chem. Soc.* **1995**, *117*, 12887–12888.
18. Weissensteiner, T.; Lanchbury, J. S. *BioTechniques* **1996**, *21*, 1102–1108.